

A robustness-oriented procedure for the design of tying reinforcement in precast concrete hollow-core floors

Simone Ravasini^{a,*}, Beatrice Belletti^a, Bassam A. Izzuddin^b, Antonello Gasperi^c

^a University of Parma, Department of Engineering and Architecture, Parco Area delle Scienze 181/A, 43124 Parma, Italy

^b Imperial College London, Department of Civil and Environmental Engineering, London SW7 2AZ, United Kingdom

^c Consulting Engineer, Modena, Italy

ARTICLE INFO

Keywords:

Progressive collapse
Robustness-oriented design
Precast concrete
Tying reinforcement
Hollow-core floor

ABSTRACT

Buildings may be subjected during their service life to extreme events which can trigger progressive collapse. On this front, the role played by tying reinforcement in structural members is crucial for an adequate load redistribution and the avoidance of disproportionate collapse. This work proposes a robustness-oriented procedure for the design of tying reinforcement placed in the hollow-core units and beams of precast concrete buildings, where limited studies are available in scientific literature. In particular, the aim is to provide a simple yet reliable approach for the design of concentrated and distributed ties in precast floors by adopting fundamental input parameters such as the system's chord rotation capacity and dynamic amplification factor, which are not considered in current design codes. Firstly, a flow-chart of the design procedure is proposed and discussed. Secondly, the input parameters are calculated based on recent analytical approaches - proposed by some of the authors - to optimize the tying reinforcement design. Finally, the efficiency of the design procedure is demonstrated with an application example, and a novel detailing scheme is proposed which is aimed at a significant enhancement of structural robustness. Due to its simplicity, the proposed design procedure is contended to be applicable in robustness assessment and design of building structures with precast concrete hollow-core floors.

1. Introduction

After the partial collapse of the Ronan Point building in London, 1968, the robustness assessment has become an important topic in structural engineering [1–3]. In this context, Codes and guidelines [4–7] provide three methods for the robustness assessment of buildings subjected to unidentified accidental actions: (i) the Tie Force (*TF*), (ii) the Alternate Load Path (*ALP*) and (iii) the Key Element methods. In the current scientific literature, limited works on precast concrete (*PC*) structures are available [8] compared with the number of studies concerning the structural robustness assessment of casted in-situ reinforced concrete structures. With the aim to avoid disproportionate collapse, the adoption of tying reinforcement in resisting *PC* members is thus crucial for an adequate load redistribution under local damage scenarios.

From the experimental point-of-view, studies aimed to investigate the progressive collapse resistance of precast concrete frames with emulative [9,10] and dry connections [11–14] are available. In particular, the latter connection type composed of beams and columns connected with steel dowels is typical of European countries [15] and

studies available in literature [11,12,16–18] highlighted the inability of dry connections to resist progressive collapse. The robustness performance of distributed ties in *PC* floors has been experimentally investigated in precast hollow-core units sub-assemblages [19–23]. In particular, Zhou et al. [23] recently tested double-span precast prestressed hollow-core units with different tying detailing, confirming that the catenary action mechanism can effectively develop at large displacements in resisting progressive collapse, as also reported in an old study from PCA [22]. The robustness performance of a real-scale *PC* structure has been experimentally investigated recently by Buitrago et al. [24,25], subjected to corner column removal.

Numerical approaches have also been considered concerning quasi-static and dynamic assessment of progressive collapse resistance of precast concrete frames [14,16,26–29], floor slabs and buildings [17, 30–33], where usually the Finite Element method or less commonly the Applied Element method are adopted. Among others, Zhou et al. [11,12] and Kim et al. [14] carried out nonlinear finite element analyses to investigate the quasi-static and dynamic response of *PC* frames with dry connections, while Tohidi et al. [34,35] and Miratashiyazdi [29] investigated the quasi-static response of double-span *HC* floor units.

* Corresponding author.

E-mail address: simone.ravasini@unipr.it (S. Ravasini).

List of symbols

T, P^*	Equivalent TF and applied loads
i_f, ρ	Intensity and reduction factors
L_l, L_t	Longitudinal and transversal span lengths
h, b, d_t	HC slab thickness, width and effective depth of distributed ties
$h_b, b_b, d_{b,t}$	PC beam height, width and effective depth of concentrated ties in beams
L_{deb}	Debonding length of distributed floor ties
$\phi_{p,b}, A_{p,t}$	Diameter and area of strands as distributed ties at each HC unit
f_c, f_{ce}, E_c	Grouting and PC member concrete compressive strengths and elastic modulus
D_L, L_L, ψ	Dead and live loads and coefficient of combination
P_0, δ_0	Gravity load and maximum displacement
E_p, E_s	Elastic modulus of strands and rebars
$f_{sp}, f_{su}, \epsilon_{su}$	Yield and ultimate tensile strengths and ultimate strain of

	bars
$f_{py}, f_{pu}, \epsilon_{pu}$	Yield and ultimate tensile strengths and ultimate strain of strands
$s_{b,u}, F_{su}$	Ultimate slip and tensile load of bars as concentrated ties in PC beams
F_{py}, F_{pu}	Yield and ultimate tensile loads of distributed floor ties
n_d, ϕ_d	Number and diameter of steel dowels in beam-to-column connections
f_{syd}, V_{Rd}	Steel dowel yield strength and shear resistance
$P_k, P_{d,k}, \delta_k$	Quasi-static and dynamic loads and displacement at event k
$M_{b,y}, P_{b,y}$	Yielding moment and load of transversal PC beams
$\delta_{b,u}, P_{b,u}$	Ultimate displacement and load of concentrated ties in PC beams
$DAF_k = \eta$	Dynamic amplification factor at event k
α_{crib}, θ_C	Critical load multiplier and chord rotation capacity
$A_{sb,b}, P_{b,c}$	Area and load contribution at catenary stage of concentrated ties in PC beams

Ravasini et al. [16] adopted a numerical approach based on fibre-based approach to simulate the dynamic responses of precast concrete frames with dry connections and the role played by concentrated tying reinforcement placed along the PC beams to mitigate progressive collapse was investigated under different column removal scenarios. A recent fragility assessment-based study [17] demonstrated that: (i) European-designed PC buildings are prone to progressive collapse and (ii) the use of only concentrated ties in beams lead to construction problems due to the considerable amount of required reinforcement. For these reasons, in a real building, both distributed ties in floors and concentrated ties in beams must be considered and simplified analytical formulations are welcome in engineering practice.

In this context, a new tying force method for robustness design of building structures has been proposed by Izzuddin & Sio [36] and validated by Ravasini et al. [37] on available experimental test results of RC structures. Moreover, a recent analytical method for the assessment of progressive collapse resistance of PC buildings with dry connections has been proposed by Ravasini [38], where both quasi-static and dynamic responses a PC system composed of distributed ties placed in HC slabs and concentrated ties placed in PC beams are analytically calculated. The method has been validated and is capable of considering the main parameters affecting the progressive collapse resistance such as the mechanical properties of tying reinforcement and concrete, and the geometrical features of PC members and the restraining stiffness. This paper proposes a robustness-oriented design procedure for concentrated and distributed tying reinforcement in PC floors realised with precast concrete hollow-core units, based on the cited analytical approaches [36,38]. The illustrated design procedure allows the optimisation of concentrated and distributed tying reinforcement in PC floors by ensuring sufficient load-bearing capacity to resist progressive collapse. The ease of use of the method is illustrated in a step-by-step calculation example, and a novel HC slabs detailing is presented, able to meet construction issues with a sufficient margin of safety.

2. Novel robustness-oriented design procedure

The Fig. 1(a) and (b) represent the views of: (i) the main geometrical features in a precast concrete (PC) building with different column removal scenarios and (ii) the distributed tying reinforcement placed in hollow-core (HC) floors and (iii) concentrated ties placed in PC beams. The distributed floor ties are placed continuously and parallel to the HC floor units (refer to Fig. 1(c), section A-A'), while the concentrated longitudinal and transversal ties are placed within the PC beams (refer to Fig. 1(d), section B-B'). Precast concrete members are completed in-situ

with concrete grouting at joints [7].

Regarding distributed ties in HC slabs, two options can be considered, refer to Fig. 1(b):

- 1) Placing of ties in voids and keyways along the span of HC floor units and grouting of voids. However, this option is more difficult to be realized in practice due to more manufacturing process and problems may arise during the placing of reinforcement. In addition, an increment of self-weight is expected due to the in-situ with concrete grouting of voids along the HC slabs.
- 2) Placing of ties along the longitudinal joints of HC floor units. This option is considered more viable since no manufacturing difficulties are expected, and because the current construction practice provides to fill transversal and longitudinal joints with concrete grouting. However, careful must be paid to the design of joints, and an ad-hoc detailing must be provided, as discussed in detail in the Section 4.

To establish adequate tying reinforcement against progressive collapse phenomenon, a rational and suitable design procedure is required to ensure that the system can withstand the applied loads after the loss of a support or load-bearing element, such as a column. On this front, a novel design procedure is proposed herein to meet such requirements, and the following steps are described in the subsequent sections:

- The flow-chart of the design procedure is described in the Section 2.1 with the main assumptions of the procedure based on the observations available in the current literature [8,39] and in the *fib* Bulletin 63 [7].
- The input parameters required for the Izzuddin & Sio proposal [36] and for application in the design procedure are reported and discussed in Section 2.2, and the analytical approach used to calculate such parameters [38] is described in Section 2.3.

2.1. Flow-chart of the design procedure and main assumptions

The flow-chart of the proposed robustness-oriented design procedure of tying reinforcement in the whole hollow-core floor system (thus, both concentrated ties in PC beams and distributed ties in HC floor units) is shown in Fig. 2. An iterative procedure is adopted to optimize the tying reinforcement system, where the main assumptions are:

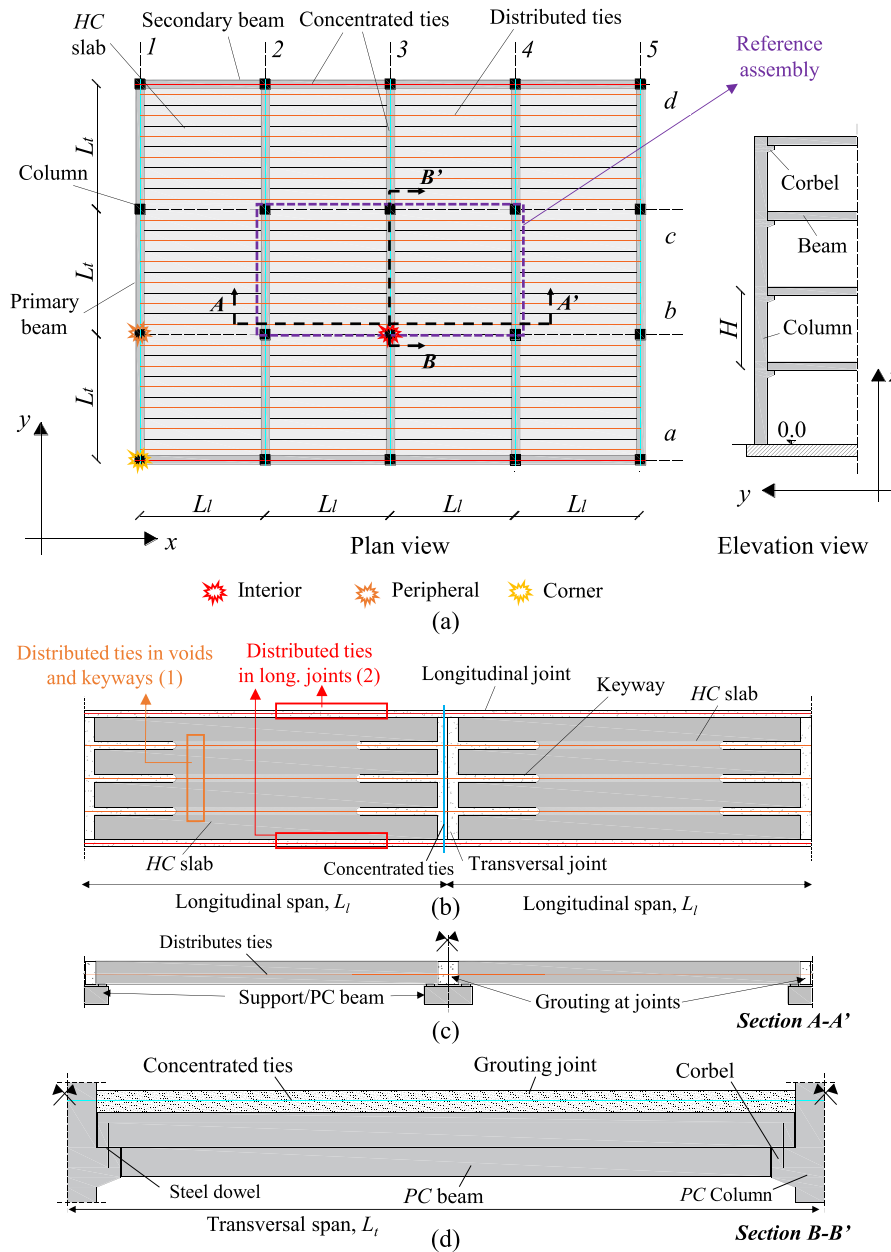


Fig. 1. Schematic view of (a), (b) PC building with column loss scenarios and distributed ties in floor slabs, (c) double-span HC floor units, (d) transversal PC beam with ties.

- The stiffness and the resistance of the system is mainly attributed to tie reinforcement placed in HC units as distributed floor ties [7]. The resistance of ties placed in PC beams are considered although its resisting contribution is limited, as discussed in the Section 2.3 and in the applicative example in the Section 3.
- The adequate connection between the concrete topping wire reinforcement and HC floor slabs is crucial to prevent progressive collapse at large displacement stage [7]. However, no experimental evidence is available in the current literature about this issue. Therefore, the resisting contribution of the wire mesh reinforcement placed in the concrete topping of HC units is neglected, since the connection may be destroyed at large displacements, if not adequately designed.
- The anchorages of beam-column connections of end-beams are assumed able to sustain redistributed loads after column loss. A posteriori check must be carried out to verify such hypothesis and to

check the occurrence of brittle failure mechanisms. Such verifications are out of the scopes of this work.

- The resistance of the whole horizontal tying system is evaluated by adding the resistance of the HC floor units and the resistance of the PC beams. To this aim the deformed shape configuration at column removal is considered to properly evaluate the displacements of HC floor units and PC beams involved in the mechanism, as discussed in the Section 2.3.
- The role played by claddings, infill walls and vertical tying systems is not considered herein, although their beneficial effects on providing additional load paths have been investigated in literature [8,40,41]

The main steps to apply the procedure are the following: (i) the definition of the geometrical features of the PC building and the mechanical properties of the reinforcement are established, (ii) the calculation of the chord rotation capacity, θ_C , and a preliminary tying reinforcement design is carried out by assuming a dynamic

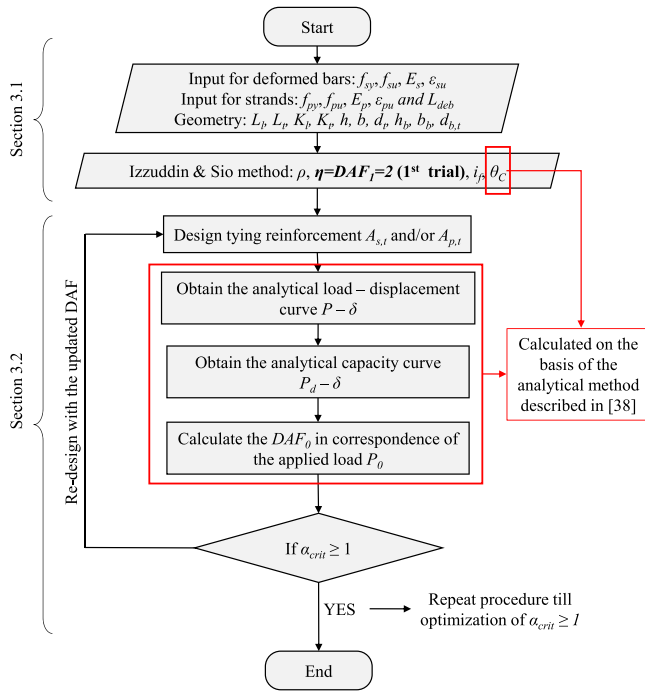


Fig. 2. Flow-chart for the robustness-oriented design procedure.

amplification factor at first trial (DAF_1) equal to 2, as proposed by Izzuddin et al. [36], since its value is not known in advance (the DAF values are iteratively updated in the following steps), (iii) the calculation of static and dynamic load-displacement curves as well as amplification factor, (iv) the applied load P_0 is compared with the resistance of the system and both DAF_0 and the critical load multiplier, α_{crit} - defined as the ratio between the maximum dynamic capacity load and the applied load - are calculated. The iterative procedure is stopped when the constraint $\alpha_{crit} \geq 1$ is achieved, implying the attainment of adequate tying reinforcement. The chord rotation capacity, the static and dynamic capacity curves and dynamic amplification factor and the critical load multiplier are calculated according to the analytical method described in [38] and reported in Section 2.3. The procedure can be adopted for both the previous options for distributed floor ties mentioned above and will be clarified in the example at the Section 3, where a step-by-step example is described to highlight the iterative nature of the proposed approach. In addition, the method is applicable in case of bars or strands used as tying reinforcement, as mentioned in [38].

As defined in the work by Ravasini [38], the chord rotation capacity is a fundamental parameter that allows the estimation of the progressive collapse performance of the system and its ductility, and is related to the ability to develop the catenary action mechanism by considering the mechanical properties of the tying reinforcement and the geometrical features.

2.2. Resisting mechanisms and definition of the input parameters

The resisting mechanisms in double-span HC units with distributed ties and subjected to central support loss have been recently observed in the experimental campaign conducted in [23], refer to Fig. 3: (A) flexural resistance, corresponding to the yielding of the ties and formation of plastic hinges due to the in-situ grouting between the HC units ($P_A-\delta_A$), (B) transitions stage, where catenary action starts ($P_B-\delta_B$) and (C) full catenary stage, where the system capacity relies only on the maximum axial tensile strength of tie reinforcements ($P_C-\delta_C$). The latter condition corresponds to the achievement of the chord rotation capacity, θ_C , calculated as the ratio between the vertical displacement, δ_C , and the longitudinal span length, L_l . Similar events are valid also for PC beams

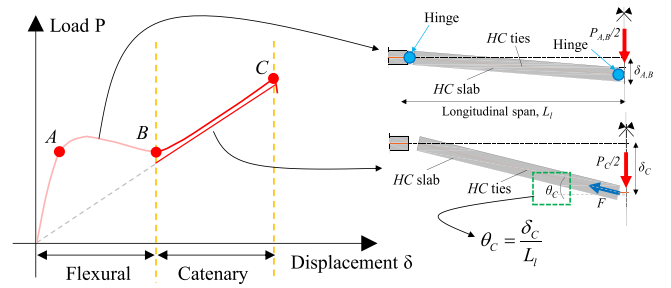


Fig. 3. Flexural and catenary stages of double-span HC units subjected to support loss.

with concentrated ties subjected to support loss.

Recently, Izzuddin & Sio [36] proposed a new tying force method for robustness design of building structures. The method is: (i) applicable in the range of catenary stage (from B to C in Fig. 3), (ii) allowing different resisting contributions of beams and floor slabs tying systems, and (iii) different types of loads can be considered according to Eq. (1):

$$T \geq \eta \rho \left(\frac{i_f}{\bar{\theta}} \right) P_0 = P^* \quad \bar{\theta} = \frac{\theta_C}{0.2} \quad (1)$$

Where P_0 is the equivalent load obtained as a superposition from all loads applied to system, T is the total equivalent tying force (TF) obtained as a superposition of the resistances of concentrated or distributed ties composing the system.

The parameters are defined as follows:

1. The term i_f is the tying force intensity factor depending on the structural configuration.
2. The term ρ is a reduction factor which allows for strain hardening and flexural/catenary interaction, which is assumed equal to 1 [36].
3. The adimensional parameter, $\bar{\theta}$, is calculated based on the chord rotation capacity, θ_C , that depends on materials properties and construction details.
4. η is the dynamic amplification factor (also reported in the following as DAF).

In correspondence of the chord rotation capacity, θ_C , representative of the system ductility, Eq. (1) allows to assess the adequacy of the provided tying system (indicated as the equivalent tying force T) to sustain the applied loads resulting from the combination of actions in accidental design situation (indicated as the equivalent load P_0).

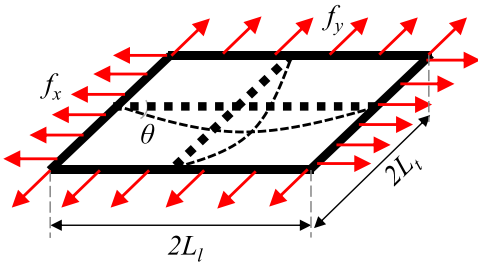
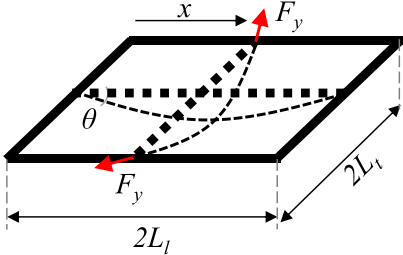
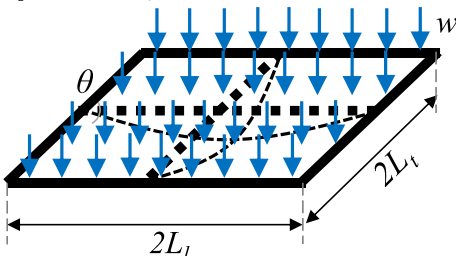
The parameters to apply the method by Izzuddin & Sio [36] are reported in Table 1:

1. The intensity factor is equal to 3.125 for two-way floor tying reinforcement.
2. The distributed tie case corresponds to ties in HC units (refer to f_x in Table 1, in [N/mm]) while the case of concentrated ties is related to ties in PC beams (refer to F_y in Table 1, in [N]), as shown in Fig. 1.
3. The chord rotation capacity, θ_C , and the dynamic amplification factor (labelled as DAF or η) are calculated in the Section 2.3.

The chord rotation capacity, θ_C , adopted in the Eq. (1), depends on mechanical properties of tying reinforcement and geometrical features, based on the deformed shape at full catenary stage shown in Fig. 4(a). As reported in [38], the chord rotation capacity has been calculated by considering the cases of rebars or strands used as distributed ties in HC floor units, also validated against experimental tests, showing good agreement.

In this work, as improvement of the previous study in [38], it is proposed to adopt partially debonded strands above supports to improve the progressive collapse resistance, as suggested in the *fib* Bulletin 63

Table 1
– Parameters for two-way floor tying reinforcement, for $L_l \leq L_t$ [36].

Equivalent tying force T	i_f
  Equivalent load P_0 	Distributed ties: $f_x L_t + f_y L_t \left(\frac{L_t}{L_l}\right)$ (In case of HC slabs along L_b , the contribution $f_y = 0$)
	3.125
	Concentrated ties: $0.9375 F_y \left(\frac{L_t}{L_l}\right) \left[\left(\frac{x}{L_l}\right) \left(2 - \frac{x}{L_l}\right)\right]^2$
	$w L_t L_t$

*Note: the load w can be calculated from the accidental load combinations from Standards

[7]. Indeed, it has been experimentally demonstrated that debonded bars can improve the progressive collapse resistance and ductility of concrete structures by avoiding excessive stress and strain localizations [23,42]. Therefore, by assuming that the elongation of the strands is explicated along the debonding length L_{deb} at both end- and mid-joints, the displacement at full catenary, δ_C , is calculated with the Eq. (2) and based on the deformed shape shown in Fig. 4(a) [38]:

$$\delta_C = \sqrt{(2\varepsilon_{pu}L_{deb} + L_l)^2 - \left(L_l - \frac{F_{pu}}{K_l}\right)^2} \quad (2)$$

Where the term F_{pu} is the axial resistance of strands, calculated with the Eq. (3):

$$F_{pu} = f_{pu}A_{p,t} \quad (3)$$

Thus, the proposed chord rotation capacity in this case is calculated with the Eq. (4):

$$\theta_C = \frac{\delta_C}{L_l} = \frac{\sqrt{(2\varepsilon_{pu}L_{deb} + L_l)^2 - \left(L_l - \frac{F_{pu}}{K_l}\right)^2}}{L_l} \quad (4)$$

The terms $A_{p,t}$ and f_{pu} are the area and maximum strength of ties in the HC unit, respectively.

The contribution provided by the restraining stiffnesses, K_l , provided by the adjacent members nearby the column loss location – through the term (F_{pu}/K_l) – is negligible in real-scale structures, and does not affect the chord rotation capacity [29,43]. The calculation of the restraining stiffness is out of the scopes of this work. The use of strands as distributed ties is justified by the following advantages: (i) strands are easy to

be placed and can be arranged along the whole span, (ii) strands provide high tensile strength, allowing the use of lower reinforcement ratios. On the other hand, the main disadvantage is the lower strands' ductility compared with rebars. However, the required ductility can be achieved by adopting an adequate debonding length, L_{deb} . This leads to an increment of the maximum elongation of ties (represented by the term $\varepsilon_{pu}L_{deb}$ in Eq. (4)), indicating that the chord rotation capacity (i.e., the system ductility) can be controlled with the selection of the debonding length. Indeed, higher the chord rotation capacity, higher the system ductility. Finally, it is worth noting that the remaining part of the ties outside of the plastic tube are bonded along the element span. Fig. 4(b) and (c) schematically represent the options mentioned in the beginning of this Section.

2.3. Calculation of the quasi-static and dynamic curves

In the following, the calculations to obtain the quasi-static static pushdown (PD) and dynamic capacity curves (CC) of the entire hollow-core floor system are briefly summarized, based on the work described in [38], where three-linear piecewise relations are adopted. Firstly, the resisting contribution provided by distributed ties in HC floor units are calculated. Secondly, the contribution of transversal concentrated ties in PC beams are calculated. Finally, the quasi-static and dynamic curves as well as the dynamic amplification factor of the entire system are obtained. It is worth noting that the dynamic amplification factor is one of the fundamental input parameters to be adopted in the Izzuddin & Sio [36] tying method. Such aspect will be clarified in the application example.

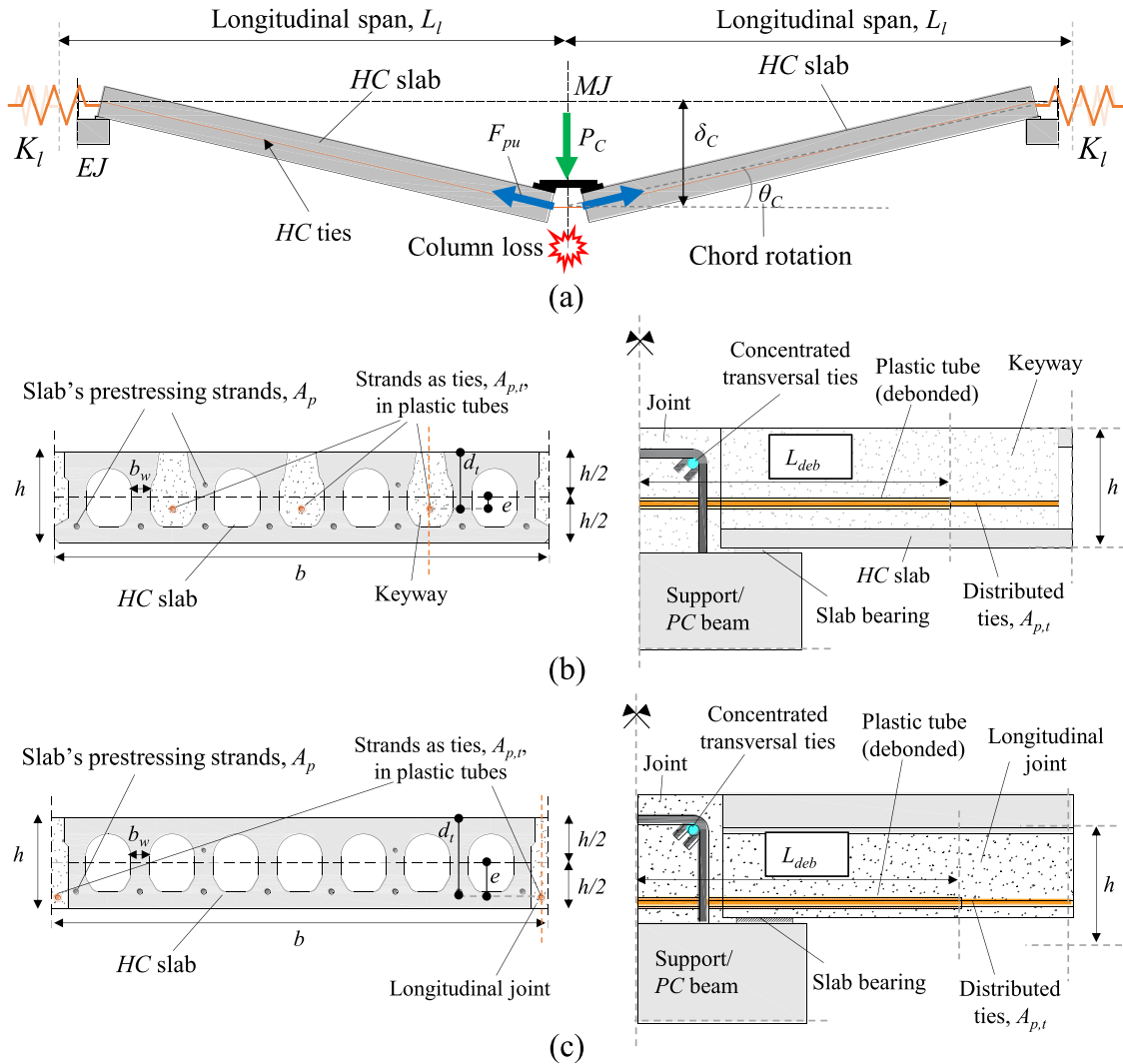


Fig. 4. (a) Deformed shape at catenary for the calculation of the chord rotation capacity [38] and (b) case of partially debonded strands as tying reinforcement, option (1), (c) case of partially debonded strands as tying reinforcement, option (2).

2.3.1. Quasi-static load-displacement curve

2.3.1.1. Resisting contributions of distributed ties in HC units. The main events occurring in double-span HC units with ties are based on the main resisting mechanisms, refer to Fig. 5(a): (A) flexural resistance, (B) transitions stage and (C) catenary stage, where the catenary action of the tie reinforcements corresponds to the achievement of maximum tensile strength. The HC slabs are considered as rigid and the nonlinearity is localized at end- and mid-joint locations (EJ and MJ, respectively), as observed from experimental and numerical studies [19,38,43,44]. The dynamic capacity curve and amplification factor are schematically represented in Fig. 5(b) and Fig. 5(c).

The vertical load at event A, P_A , is calculated with the Eq. (5), from the equilibrium condition:

$$P_A = P_B = \frac{2M_{y,MJ} + 2M_{y,EJ}}{L_l} \quad (5)$$

where $M_{y,MJ}$ and $M_{y,EJ}$ are the yielding moments at the mid- and end-joints, calculated as $M_y = 0.9f_{py}A_{p,t}d_t$. The terms d_t , $A_{p,t}$ and f_{py} represent the effective depth, area and yielding strength of strands used as ties, respectively, at each HC unit. The vertical displacement at event A, δ_A , is calculated with the Eq. (6) based on the chord rotation at ties' yielding:

$$\delta_A = \theta_y L_l = \left[\frac{M_y}{0.5E_c I} L_{deb} \right] L_l \quad (6)$$

where an average value between yielding moment at end- and mid-joints can be adopted and the cracked stiffness is assumed equal to a half of the un-cracked stiffness, while the Young's modulus E_c , has been evaluated according to Eq. (7), [45]:

$$E_c = 21500(f_c/10)^{1/3} \quad (7)$$

in which f_c is the concrete grouting compressive strength.

The displacement at event B, δ_B , is equal to the height of the HC unit, h , since it was experimentally observed the onset of catenary stage at a displacement approximately equal to the member's height [19,23,29,46]. The compressive arch action resisting contribution is neglected in virtue of the high span-to-depth ratio of HC units [47].

The vertical load at full catenary, P_C , is calculated with the Eq. (8) by considering the equilibrium in Fig. 4(a) and Fig. 5(a) and θ_c in Eq. (4):

$$P_C = 2F_{pu} \frac{\delta_c}{L_l} = 2F_{pu} \theta_c \quad (8)$$

The previous formulations have been extended in the case of an entire hollow-core floor system, Fig. 1, where the reference assembly is indicated. The basic idea to obtain the whole load-displacement

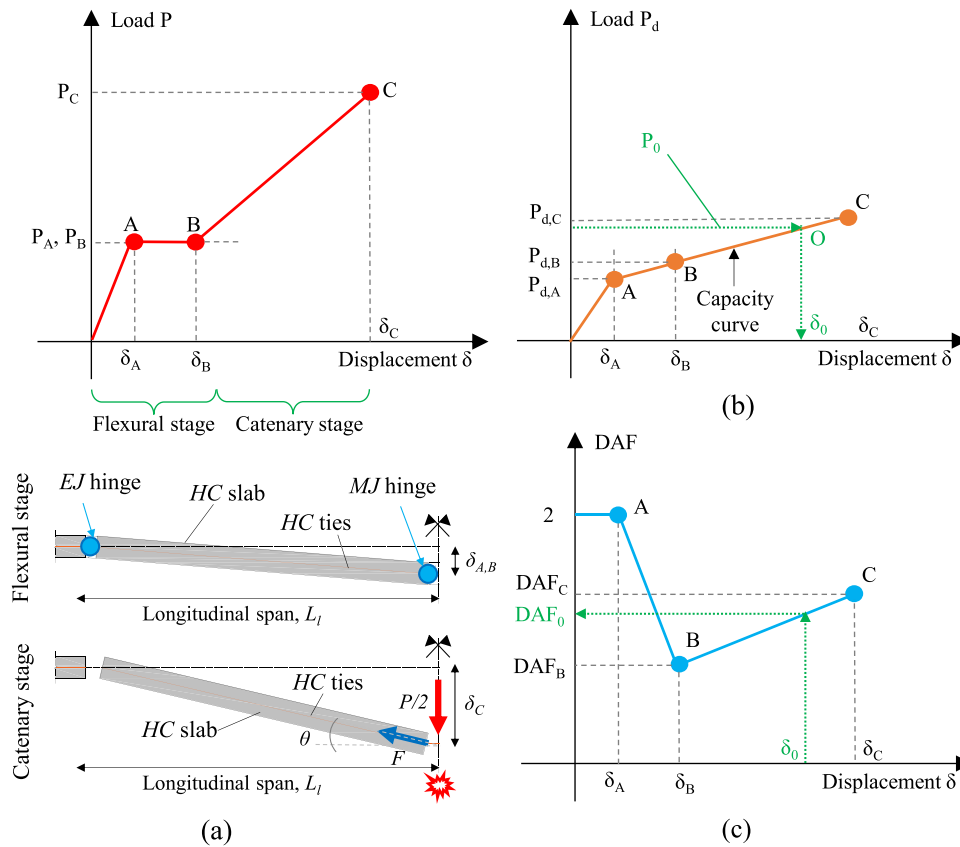


Fig. 5. Double-span HC units: (a) quasi-static load-displacement curve, (b) dynamic capacity curve and (c) dynamic amplification factor, refer also to [38].

response is to superimpose the resisting contributions of the distributed ties in “J” slab units by calculating ties displacements proportionally to the displacement at column loss location, δ , as shown in Fig. 6. The resistance P_k at displacements δ_k (with event $k = A, B$ and C) for distributed ties in hollow-core units is calculated by using the Eq. (9):

$$P_k = n_{\text{sys}t} \sum_{i=1}^J P_i(\delta_i) \quad \text{where} \quad \begin{cases} k = A, B, C \\ i = i\text{-th HC unit} \\ J = \# \text{ of double-span HC units} \end{cases} \quad (9)$$

The parameter $n_{\text{sys}t}$ depends on the column removal location (Fig. 1): (i) 2 for interior column loss, (ii) 1 for peripheral edge column loss and (iii) 0.5 for corner column loss.

2.3.1.2. Resisting contributions of concentrated ties in PC beams. The flexural and catenary resisting contributions provided by ties placed in PC beams are similar to those described for double-span HC units in Section 2.3.1.1.

The flexural resistance provided by concentrated ties in PC beams is calculated with the Eq. (10), [30,38], based on the work by El-debs et al. [48] and Elliot et al. [49,50]:

$$P_{b,y} = \frac{2M_{b,y,MJ} + 2M_{b,y,EJ}}{L_t} = \frac{2}{L_t} [V_{Rd}y_d + f_{sy}A_{sb,t}y_{b,t}] = \frac{2}{L_t} \left[V_{Rd} \left(h_b - 0.5 \frac{V_{Rd}}{b_h f_c} \right) + f_{sy}A_{sb,t} \left(d_{b,t} - \frac{0.45f_{sy}A_{sb,t}}{0.67 \cdot 0.9f_c b_b} \right) \right] \quad (10)$$

Where V_{Rd} is the steel dowel shear resistance [51], calculated as $V_{Rd} = n_d \phi_d^2 \sqrt{f_{ce} f_{syd}}$. The terms are: n_d , ϕ_d and f_{syd} are the number, diameter, and yield strength of the dowel and f_{ce} and f_{ce} are the concrete compressive strength of grouting and PC elements. The term b_b is the width of the beam, h_b is the height of beam-end, while $M_{b,y,MJ}$ and $M_{b,y,EJ}$ are the yielding moments at mid-joint and end-joints, as shown in Fig. 7. The contribution at catenary stage of concentrated ties, $P_{b,c}$, is proportional to the displacement of slabs at column loss with the Eq. (11):

$$P_{b,c} = P_{b,y} + \frac{(P_{b,u} - P_{b,y})}{(\delta_{b,u} - \delta_B)} (\delta_C - \delta_B) \quad (11)$$

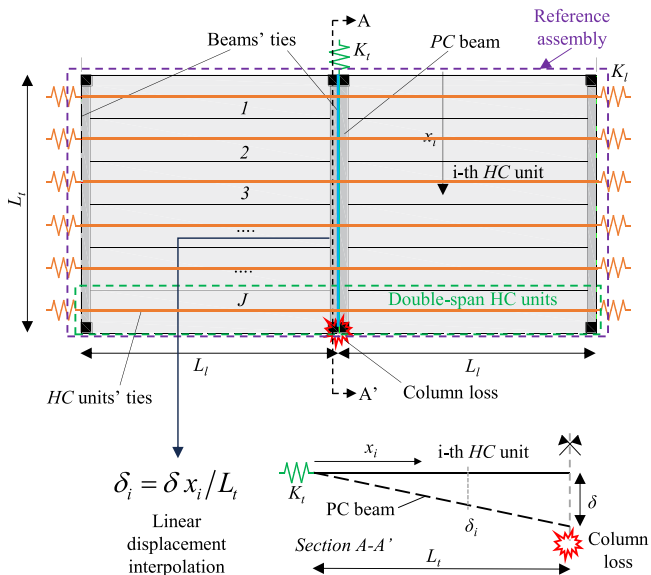


Fig. 6. Displacement interpolation in the HC floor with slabs and beams, refer also to [38].

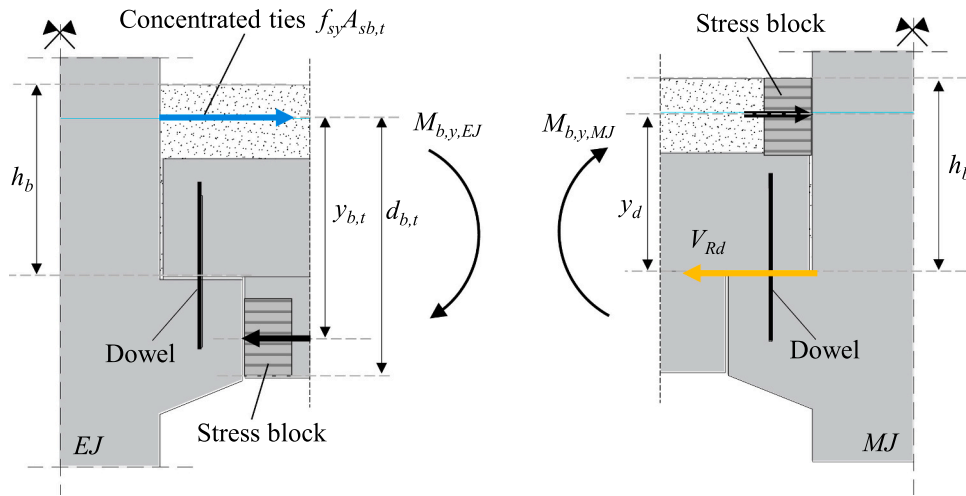


Fig. 7. Negative and positive moments [48–50] at yielding, used in [30,38].

The displacement $\delta_{b,u}$ of concentrated ties in PC beams is calculated with the Eq. (12):

$$\delta_{b,u} = \sqrt{(2s_{b,u} + L_t)^2 - \left(L_t - \frac{F_{su}}{K_t}\right)^2} \quad (12)$$

The slip of the ties in PC beams, $s_{b,u}$, in correspondence of the bar fracture, is calculated with the model by Feng & Xu [52] with the Eq. (13):

$$s_{b,u} = \frac{\varepsilon_{sy} f_{sy} \phi_{b,t}}{2 \cdot 4\sqrt{f_c}} + \frac{(\varepsilon_{su} + \varepsilon_{sy})}{2} \frac{(f_{su} - f_{sy}) \phi_{b,t}}{4 \cdot 0.5\sqrt{f_c}} \quad (13)$$

The load at full catenary of concentrated ties in PC beam is calculated with the Eq. (14):

$$P_{b,u} = 2F_{su} \frac{\delta_{b,u}}{L_t} = 2(A_{sb,t} f_{sy}) \frac{\delta_{b,u}}{L_t} \quad (14)$$

The final displacement of the system is attributed to the minimum of the ultimate displacements of the HC floor units and the transversal PC beams, in Eq. (2) and Eq. (12), respectively. The load $P_{b,u}$ is calculated with the Eq. (8), by using the geometrical and mechanical properties of concentrated ties in beams (where $F_{su} = A_{sb,t} f_{su}$) and the span L_t .

Finally, the total quasi-static pushdown load of the system is the sum of Eqs. (9) and (10) for the events A, B and of the Eqs. (9) and (11) for the event C. It is worth to state that, depending on the column loss scenario (Fig. 1), the PC system is assumed to provide the following resisting mechanisms:

- In the case of interior column removal scenario (Fig. 1), the system relies its resistance on both flexural and catenary action resisting contributions, thus all the main events can be attained (from A to C).
- In the case of peripheral edge column removal scenario (Fig. 1), the system relies its resistance on the maximum between its flexural resistance and the catenary resistance of concentrated ties in PC beams, with no resisting contribution of ties in HC units due to lack of continuity. However, since the resisting contribution of concentrated ties in beams may be inhibited due to insufficient restraining, it is conservatively assumed to rely only on the flexural resistance of the slabs and beams, where the maximum system’s capacity in terms of load and displacement are associated to the achievement of the event B. The same assumption is valid for the corner column removal scenario.

2.3.2. Dynamic load-displacement curve

The dynamic load-displacement curve, so-called pseudo-static

response [49], is calculated with the energy conservation principle [53, 54], and the expressions are reported in the Eq. (15), Fig. 5(b):

$$\begin{cases} P_{d,A} = \frac{1}{2} P_A \\ P_{d,B} = \frac{1}{2\delta_B} [P_A \delta_A + (P_A + P_B)(\delta_B - \delta_A)] \\ P_{d,C} = \frac{1}{2\delta_C} [P_A \delta_A + (P_A + P_B)(\delta_B - \delta_A) + (P_B + P_C)(\delta_C - \delta_B)] \end{cases} \quad (15)$$

The critical load multiplier, α_{crit} , is a robustness indicator and is defined as the ratio between the pseudo-static capacity, $P_{d,k}$, and the applied load, P_0 , which presents a rational measure of robustness [49]:

$$\alpha_{crit} = \frac{\max(P_{d,k})}{P_0} \quad k = A, B, C \quad (16)$$

If α_{crit} results greater or equal than 1, the system can sustain the loss of the load bearing element, otherwise, the system collapses. If α_{crit} is equal to 1, the system is at incipient collapse. In other words, if the applied load P_0 intersect the dynamic capacity curve, Fig. 5(b), the system can sustain the loss of the load bearing element and the maximum displacement, δ_0 , is obtained.

Finally, the Dynamic Amplification Factor (DAF) [55] is calculated with the Eq. (17):

$$\begin{cases} DAF_A(\delta_A) = \frac{P_A}{P_{d,A}} = 2 \quad \text{for } 0 \leq \delta \leq \delta_A \\ DAF_B(\delta_B) = \frac{P_B}{P_{d,B}} = \frac{2\delta_B P_B}{[P_A \delta_A + (P_A + P_B)(\delta_B - \delta_A)]} \\ DAF_C(\delta_C) = \frac{P_C}{P_{d,C}} = \frac{2\delta_C P_C}{[P_A \delta_A + (P_A + P_B)(\delta_B - \delta_A) + (P_B + P_C)(\delta_C - \delta_B)]} \end{cases} \quad (17)$$

The DAF_0 , corresponding to the load P_0 , is determined from the intersection, see Fig. 5(c).

It is worth to state that, to better discretize the load-displacement capacity and DAF curves, intermediate points can be adopted between the events A, B, C, as described in [38].

3. Application example and discussion

An example is described herein with the step-by-step application of the proposed design procedure in the case of interior column loss. The results are thus compared with the minimum TF requirements from Eurocode 1 and 2.

3.1. Geometrical and mechanical features

The geometrical features of the PC building reported in Fig. 1 are referred to previous works [17,30] and are summarized in Table 2. The number of HC slabs, J , of the reference system is equal to nine, so giving a transversal span length, L_t , of $9 \times 1.2 = 10.8$ m, while the longitudinal span, L_l , is equal to 7.2 m. The compressive strengths of concrete grouting at joints, f_c , and PC elements, f_{ce} , are equal to 30 and 50 MPa, respectively, and the properties of ties are shown in Table 3. Precast concrete beams and columns are connected with one steel dowel of diameter 18 mm [30]. For simplicity, the ties of the HC slabs are placed at half of the element height ($d_t = 110$ mm) and the effective depth of beam, $d_{b,b}$, is equal to 850 mm. For details concerning the geometry of slabs and beam, refer to Fig. 8, Fig. 4(b) and Fig. 7.

The accidental load combination and the combination coefficient, ψ , equal to 0.5, from the Eurocode 0 [56], have been adopted. The dead and live loads, D_L (3.5 kN/m² of HC slab and RC topping weights and 0.5 kN/m² for floor equipment) and L_L , are equal to 4 kN/m² and 4 kN/m², respectively. By considering also the transversal beam weight, W_b , roughly equal to 8 kN/m \times 10.8 = 86.4 kN [17,30], the load, P_0 , in accidental design situation results equal to:

$$P_0 = wL_tL_l + W_b = (D_L + \psi L_L)L_tL_l + W_b = (4.0 + 0.5 \cdot 4.0) \cdot 10.8 \cdot 7.2 + 86.4 = 552.96 \text{ kN}$$

3.2. Procedure for design of tying reinforcement

In the following, the procedure summarised in the flow-chart illustrated in Fig. 2 is reported. The main steps are described in detail with the formulations reported in the Section 2.3.

3.2.1. Preliminary design of tying reinforcement

In this step, the Izzuddin & Sio formulation reported in the Eq. (1) is applied with a $DAF = \eta = 2$, $\rho = 1$, and the chord rotation capacity of strands, calculated according to Eq. (2) as:

$$\theta_C = \frac{\sqrt{(2\varepsilon_{pu}L_{deb} + L_t)^2 - (L_t)^2}}{L_t} = \frac{\sqrt{(2 \cdot 0.035 \cdot 350 + 7200)^2 - (7200)^2}}{7200} = 0.0826 \text{ rad}$$

The equivalent load is calculated with the Eq. (1) and becomes:

$$T \geq \eta\rho \left(\frac{i_f}{\theta}\right) P_0 = 2 \cdot 1 \cdot \left(\frac{3.125}{0.0826/0.2}\right) \cdot 552.96 = 8371.49 \text{ kN}$$

Where the equivalent tying resistance, T , is calculated by summing the resisting contributions of ties placed in beams and slab units indicated as T_1 and T_2 , respectively. By assuming (1) three 28-mm bars in PC beams and (2) three 15.7-mm strands (each strand's area equal to 150 mm²) in each HC unit, the contributions are calculated with yield strengths and $x = 0.5L_t$:

$$T_1 = 0.9375F_y \left(\frac{L_t}{L_t}\right) \left[\left(\frac{x}{L_t}\right) \left(2 - \frac{x}{L_t}\right)\right]^2 = 0.9375 \cdot 2 \cdot \frac{\pi \times 28^2}{4} \cdot 450 \cdot \left(\frac{7.2}{10.8}\right) \cdot 0.75^2 = 292.24 \text{ kN}$$

Table 2
– Geometry of HC slabs and PC beams.

PC member	h (h_b) [mm]	b (b_b) [mm]	L_t [m]	L_{deb} [mm]	L_l [m]	d_t [mm]	$d_{b,t}$ [mm]
HC slab	220.0 (-)	1200.0 (-)	-	350.0	7.2	110.0	-
Transversal PC beam	- (580.0)	- (500.0)	10.8	-	-	-	850.0

$$T_2 = f_t L_t + f_y L_l \left(\frac{L_t}{L_t}\right) = \left(\frac{3 \cdot 150 \cdot 1670}{1000}\right) \cdot (1000 \cdot 10.8) + 0 = 8116.20 \text{ kN}$$

The total equivalent tying force T results equal to 8408.44 kN, higher than the required equivalent load. It can be observed that $T_2 \gg T_1$, indicating the predominant role played by distributed floor ties in resisting progressive collapse. However, the concentrated ties placed in beams allow the redistribution to adjacent members and must be adopted [7,51]. Note also that the design of ties with the equivalent tying force T , Eq. (1), has been carried out by conservatively considering the yielding strength [36].

3.2.2. Calculation of the system resistance

The resistance of the HC floor system is established as follows.

3.2.2.1. Calculation of the pushdown curve of double-span HC floor units.

The yielding moment of the HC slab sections is calculated as in Section 2.3:

$$M_y = 0.9f_{py}A_{p,t}d_t = 0.9 \cdot 110 \cdot 3 \cdot 150 \cdot 1670 = 74.40 \text{ kN}\cdot\text{m}$$

Note that yielding moments and end- and mid-joints are almost equal since ties are assumed to be placed at half of HC height. The corresponding load is calculated with the Eq. (5):

$$P_A = P_B = \frac{4M_y}{L_t} = \frac{4 \cdot 74.4}{7.2} = 41.33 \text{ kN}$$

The elastic modulus of the concrete grouting is calculated with the Eq. (7) resulting equal to 31008.37 MPa. The second moment of inertia, I , is calculated with an equivalent I -shaped section for HC slabs with $b_w = 450$ mm and top and bottom flanges equal to 40 mm, resulting in $I = 8.93 \cdot 10^8$ mm⁴. The displacement at yielding, δ_A , is thus calculated with the Eq. (6):

$$\delta_A = \theta_y L_t = \left[\frac{M_y}{0.5E_c I_{deb}}\right] L_t = \left(\frac{74.40 \cdot 10^6}{0.5 \cdot 31008.37 \cdot 8.93 \cdot 10^8}\right) \cdot 350 = 13.54 \text{ mm}$$

The displacement at event B, δ_B , is equal to 220 mm. The displacement at catenary stage, δ_C , is calculated with the Eq. (2):

$$\delta_C = \sqrt{(2\varepsilon_{pu}L_{deb} + L_t)^2 - (L_t)^2} = \sqrt{(2 \cdot 0.035 \cdot 350 + 7200)^2 - (7200)^2} = 594.47 \text{ mm}$$

The corresponding load is calculated with the Eq. (8):

$$P_C = 2F_{pu} \frac{\delta_C}{L_t} = 2 \cdot 1860 \cdot 3 \cdot 150 \cdot \frac{594.47}{7200} = 138.22 \text{ kN}$$

3.2.2.2. Calculation of resisting contributions of PC beams.

The shear resistance of the steel dowel, V_{Rd} , is calculated as:

$$V_{Rd} = n_d \alpha \phi_d^2 \sqrt{f_{ce} f_{syd}} = 1 \cdot 1 \cdot 18^2 \cdot \sqrt{50 \cdot 450} = 48.60 \text{ kN}$$

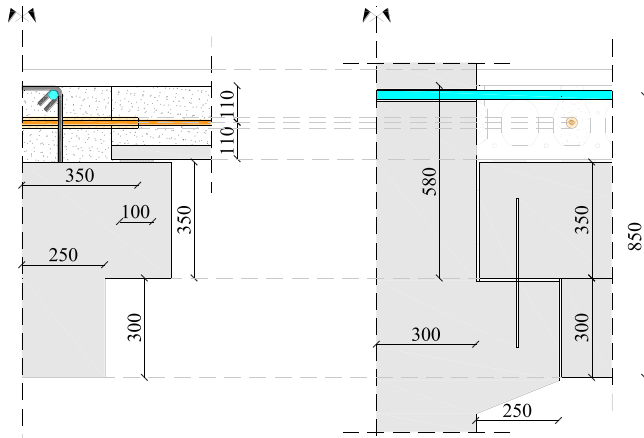
The load at yielding of ties in PC beam, $P_{b,y}$, is calculated with the Eq. (10), [30,38]:

$$P_{b,y} = \frac{2}{L_t} \left[V_{Rd} \left(h_b - 0.5 \frac{V_{Rd}}{b_n f_c} \right) + f_{sy} A_{sb,t} \left(d_{b,t} - \frac{0.45 f_{sy} A_{sb,t}}{0.67 \cdot 0.9 f_c b_b} \right) \right] = \frac{2}{10800} \left[48600 \cdot \left[580 - 0.5 \frac{48600}{500 \cdot 30} \right] + \frac{450 \cdot 3 \cdot \pi \cdot 28^2}{4} \cdot \left[850 - \frac{0.45 \cdot 450 \cdot 3 \cdot \frac{\pi \cdot 28^2}{4}}{0.60 \cdot 30 \cdot 500} \right] \right] = \frac{2}{10800} \cdot [28.11 + 672.02] \cdot 10^6 = 129.63 \text{ kN}$$

Table 3

– Mechanical properties of tying reinforcement.

Tying reinforcement	Rebars (in beams)				Strands (in slab units)			
	f_{sy} [MPa]	f_{su} [MPa]	E_s [GPa]	ϵ_{su} [%]	f_{py} [MPa]	f_{pu} [MPa]	E_p [GPa]	ϵ_{pu} [%]
Properties:	450.0	540.0	200.0	0.075	1670.0	1860.0	195.0	0.035

**Fig. 8.** Details of HC slabs and PC beams for the example. Dimensions in [mm].

Note that the resisting contribution provided by dowels is very low and, in practical applications, could be neglected. The ultimate slip of the ties, $s_{b,u}$, is calculated with Eq. (13):

$$s_{b,u} = \frac{\epsilon_{sy} f_{sy} \phi_{b,t}}{2 \cdot 4 \sqrt{f'_c}} + \frac{(\epsilon_{su} + \epsilon_{sy})}{2} \cdot \frac{(f_{su} - f_{sy}) \phi_{b,t}}{4 \cdot 0.5 \sqrt{f'_c}} =$$

$$= 0.5 \cdot \frac{450}{200000} \cdot \frac{450 \cdot 28}{4 \cdot \sqrt{30}} + 0.5 \cdot \left(\frac{450}{200000} + 0.075 \right) \cdot \frac{(540 - 450) \cdot 28}{4 \cdot 0.5 \cdot \sqrt{30}} = 9.53 \text{ mm}$$

Thus, the catenary displacement and load, $\delta_{b,u}$ and $P_{b,u}$, are calculated with Eqs. (12) and (14):

$$\delta_{b,u} = \sqrt{(2s_{b,u} + L_t)^2 - (L_t)^2} = \sqrt{(2 \cdot 9.53 + 10800)^2 - (10800)^2}$$

$$= 642.0 \text{ mm}$$

$$P_{b,u} = 2 \cdot \left(3 \cdot \pi \frac{28^2}{4} \right) \cdot 540 \cdot \left(\frac{642.0}{10800} \right) = 118.53 \text{ kN}$$

Since $\delta_{b,u} > \delta_C$, the failure of the system is attributed to the fracture of ties in HC units.

3.2.2.3. Calculation of the pushdown curve of the HC floor system. The system's load-displacement curve is calculated with a linear interpolation and the contributions of HC floors with the Eq. (9), and shown in Fig. 6. The loads ad events A, B and C attributed to the HC floor units are summed as follows, where n_{syst} is equal to 2:

$$P_A = n_{syst} \sum_{i=1}^9 P_{A,i} =$$

$$2 \cdot (4.59 + 9.19 + 13.78 + 18.37 + 22.96 + 27.56 + 32.15 + 36.74 + 41.33) =$$

$$= 2 \cdot 206.67 = 413.34 \text{ kN}$$

$$P_B = n_{syst} \sum_{i=1}^9 P_{B,i} =$$

$$= 2 \cdot (41.33 + 41.33 + 41.33 + 41.33 + 41.33 + 41.33 + 41.33 + 41.33 + 41.33) =$$

$$= 2 \cdot 371.99 = 743.98 \text{ kN}$$

$$P_C = n_{syst} \sum_{i=1}^9 P_{C,i} =$$

$$= 2 \cdot (41.33 + 41.33 + 41.33 + 52.77$$

$$+ 69.86 + 86.95 + 104.04 + 121.13 + 138.22) =$$

$$= 2 \cdot 696.96 = 1393.92 \text{ kN}$$

The results from interpolation are summarized in Table 4.

The catenary contribution of the PC beam's ties is proportional to the HC floor displacement, calculated with the Eq. (11):

$$P_{b,c} = P_{b,y} + \frac{(P_{b,u} - P_{b,y})}{(\delta_{b,u} - \delta_B)} (\delta_C - \delta_B)$$

$$= 89.57 + \frac{(118.53 - 89.57)}{(642.0 - 220.0)} (594.47 - 220.0) = 119.78 \text{ kN}$$

Finally, the total quasi-static load of the HC floor system is updated with the PC beams' resisting contributions:

$$P_A = 413.33 + 129.63 = 542.96 \text{ kN}$$

$$P_B = 743.98 + 129.63 = 873.61 \text{ kN}$$

$$P_C = 1393.91 + 119.78 = 1513.69 \text{ kN}$$

3.2.2.4. Calculation of the capacity curve, critical load multiplier and amplification factor. The dynamic capacity curve is calculated as reported in the Eq. (15):

$$\left\{ \begin{array}{l} P_{d,A} = \frac{1}{2} P_A = \frac{1}{2} 542.96 = 271.48 \text{ kN} \\ P_{d,B} = \frac{1}{2 \delta_B} [P_A \delta_A + (P_A + P_B) (\delta_B - \delta_A)] = \\ \quad = \frac{1}{2 \cdot 220.00} [542.96 \cdot 13.54 \\ \quad + (542.96 + 873.61) \cdot (220.00 - 13.54)] = 681.40 \text{ kN} \\ P_{d,C} = \frac{1}{2 \delta_C} [P_A \delta_A + (P_A + P_B) (\delta_B - \delta_A) + (P_B + P_C) (\delta_C - \delta_B)] = \\ \quad = \frac{1}{2 \cdot 594.47} [542.96 \cdot 13.54 + (542.96 + 873.61) \cdot (220.00 - 13.54) + \\ \quad + (873.61 + 1513.69) \cdot (594.47 - 220.00)] = 1004.08 \text{ kN} \end{array} \right.$$

The critical load multiplier, α_{crit} , is determined by the ratio between the maximum dynamic load (where $k = A, B, C$) and the applied load P_0 :

$$\alpha_{crit} = \frac{\max(P_{d,k})}{P_0} = \frac{1004.08}{552.96} = 1.82$$

Therefore, since it is greater than 1 (i.e., $P_0 < P_{d,C}$), the system is able to sustain the gravity load P_0 after the column loss. Finally, the dynamic amplification factor is calculated with the Eq. (17):

$$\left\{ \begin{array}{l} DAF_A(\delta_A) = \frac{P_A}{P_{d,A}} = 2 \quad \text{for } 0 \leq \delta \leq \delta_A \\ DAF_B(\delta_B) = \frac{P_B}{P_{d,B}} = \frac{873.61}{681.40} = 1.28 \\ DAF_C(\delta_C) = \frac{P_C}{P_{d,C}} = \frac{1513.69}{1004.08} = 1.51 \end{array} \right.$$

And both the displacement under applied load P_0 , δ_0 , and the DAF_0

Table 4

– Displacement and load interpolation of HC floor units of the reference assembly.

HC units:	#1	#2	#3	#4	#5	#6	#7	#8	#9
x_i [m]	1.20	2.40	3.60	4.80	6.00	7.20	8.40	9.60	10.80
$\delta_{A,i}$ [mm]	1.50	3.01	4.51	6.02	7.52	9.02	10.53	12.03	13.54
$P_{A,i}$ [kN]	4.59	9.19	13.78	18.37	22.96	27.56	32.15	36.74	41.33
$\delta_{B,i}$ [mm]	24.44	48.89	73.33	97.78	122.22	146.67	171.11	195.56	220.00
$P_{B,i}$ [kN]	41.33	41.33	41.33	41.33	41.33	41.33	41.33	41.33	41.33
$\delta_{C,i}$ [mm]	66.05	132.11	198.16	264.21	330.26	396.32	462.37	528.42	594.47
$P_{C,i}$ [kN]	41.33	41.33	41.33	52.77	69.86	86.95	104.04	121.13	138.22

are calculated based on the intersections shown in Fig. 5 and by using a simple linear interpolation.

3.2.3. Iterative procedure and optimization of tying reinforcement

The tying reinforcement can be optimized by using the updated DAF (at the end of the previous calculation steps, equal to 1.20 from a linear interpolation by intersecting the load P_0 with the DAF plot). With this new value, the ties are re-designed in the iteration #2 by adopting the Eq. (1) and the procedure continues till the optimisation of the critical load multiplier is achieved. Table 5 reports the iterations and the corresponding DAFs, maximum displacements, tying reinforcement and critical load multipliers. The graphical results of the procedure are summarized in Fig. 9 in terms of pushdown (PD) load-displacement relation and capacity curve (CC) as well as DAF.

Similar calculations can be performed by considering the absence of concrete grouting at joints, although it leads to a more punitive verification of the system in virtue of the consequent higher dynamic amplification factors, as described and discussed in [38]. However, grouting of joints is a well-consolidated construction practice [7,51] and its beneficial resisting contribution must be adequately considered. Also, the use of rebars as distributed ties in HC floor units and/or the use of strands as concentrated ties in beams are permitted by following a similar procedure.

Note that the displacement δ_0 , derived from the intersection of the capacity curve with the accidental load P_0 , corresponds to the maximum displacement at transient state achieved by the system after the support loss.

Table 5

– Main results of the proposed procedure.

Iteration	Calculated from the Izzuddin proposal[36,37].			Calculated from the analytical approach, further details in[38]		
	P^* [kN]	Tying reinforcement [mm ²]	$T_1+T_2 = T$ [kN]	α_{crit} [/]	δ_0 [mm]	DAF (=η) [/]
#1 (η = 2)	8371.49	3 φ28 bars in beams + 3 φ15.7 strands in HC slab	292.24 + 8116.20 = = 8408.44	1.82	89.08	1.20
#2 (η = DAF #1)	5022.89	2 φ26 bars in beams + 3 φ15.2 strands in HC slab	167.99 + 7521.01 = 7689.00	1.61	171.24	1.26
#3 (η = DAF #2)	5274.04	2 φ26 bars in beams + 2 φ15.7 strands in HC slab	167.99 + 5410.80 = 5578.79	1.20	400.37	1.41

Note: $P_0 = 552.96$ kN, $i_f = 3.125$, $\delta_C = 594.47$ mm, $\theta_C = 0.0826$ rad.

3.3. Comparisons with current Eurocodes provisions

In the context of progressive collapse resistance, the ties placed in the PC members and at each HC unit can be designed according to the Eurocode 1 and 2 [5,6]. From Eurocode 1 [5], the calculations of the minimum tensile force to be sustained by concentrated ties in beams and distributed at each HC slab unit, respectively, are:

$$T_{i,b} \geq \max[0.8 \cdot L_t \cdot L_i (D_L + \psi L_L); 75] = \max[373.25; 75] = 373.25 \text{ kN}$$

$$T_{i,HC} \geq \max[0.8 \cdot b \cdot L_i (D_L + \psi L_L); 75] = \max[67.39; 75] = 75 \text{ kN}$$

Eurocode 2 [6] provides the following minimum requirements for ties in beams and floors, respectively:

$$T_{i,b} \geq \max \left[20 \cdot \frac{L_t + L_i}{2}; 70 \right] = \max[180; 70] = 180 \text{ kN}$$

$$T_{i,HC} \geq 20 \text{ kN/m}$$

To satisfy the minimum Eurocode requirements, it is sufficient to use two 26-mm bars in PC beams and one 9.3-mm strand (52 mm² area) at each HC unit. Fig. 10 shows the comparisons of the pushdown and capacity curves calculated with the analytical method (Section 2.3) by considering the tying reinforcement designed with the proposed procedure and Eurocodes. In the latter case, it is evident a considerable loss in the load-bearing capacity of the system (Fig. 10(a)) and the inability to redistribute the loads, as evidenced by the absence of intersection with the capacity curve, Fig. 10(b). Indeed, the critical load multipliers result equal to 1.20 and 0.32 in case of proposed design procedure and Eurocodes, respectively.

The main differences are attributed to the following aspects:

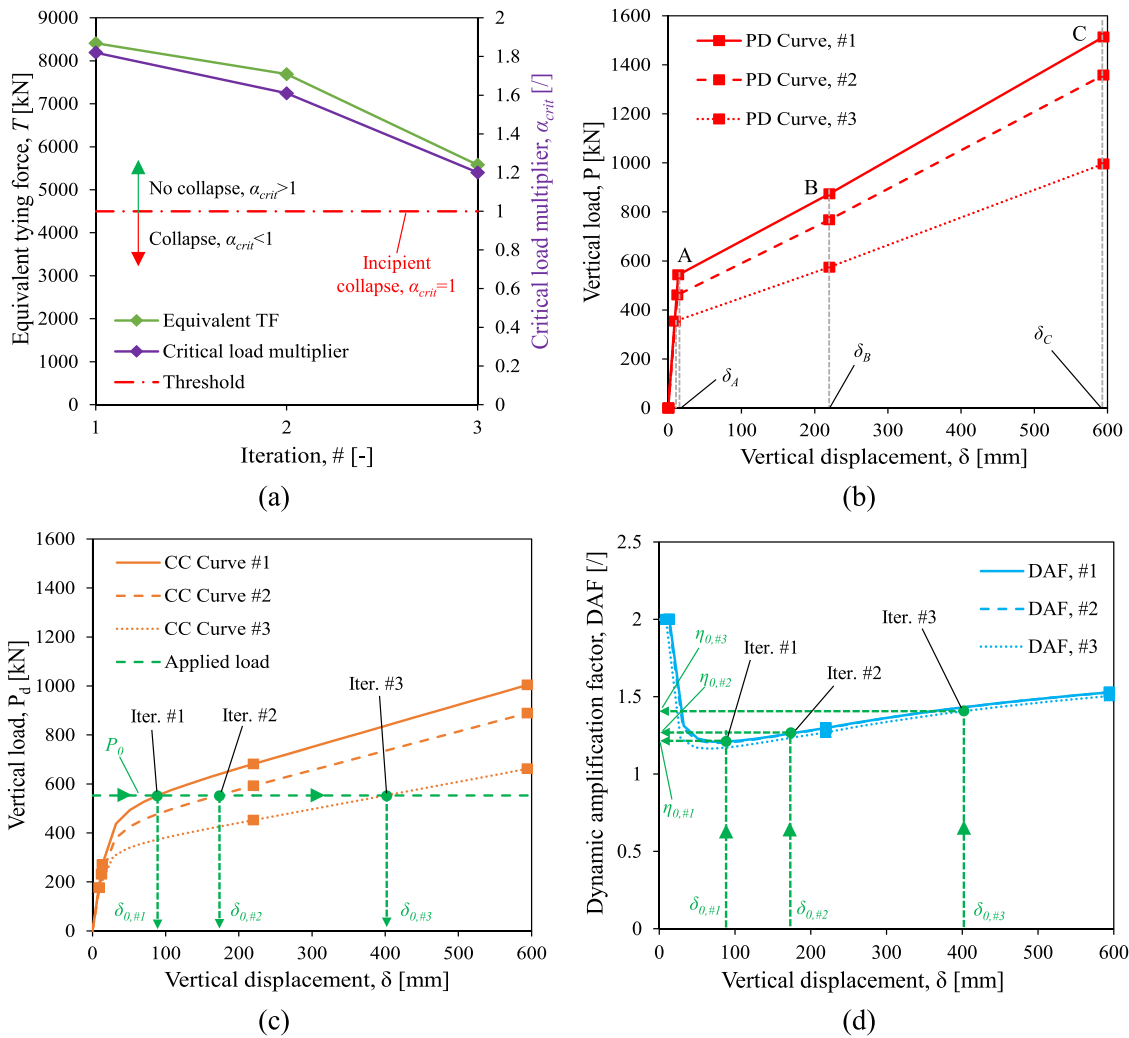


Fig. 9. Results from the proposed procedure: (a) Variation of α_{crit} and equivalent TF with iterations, (b, c, d) pushdown, capacity curves and dynamic amplification factors.

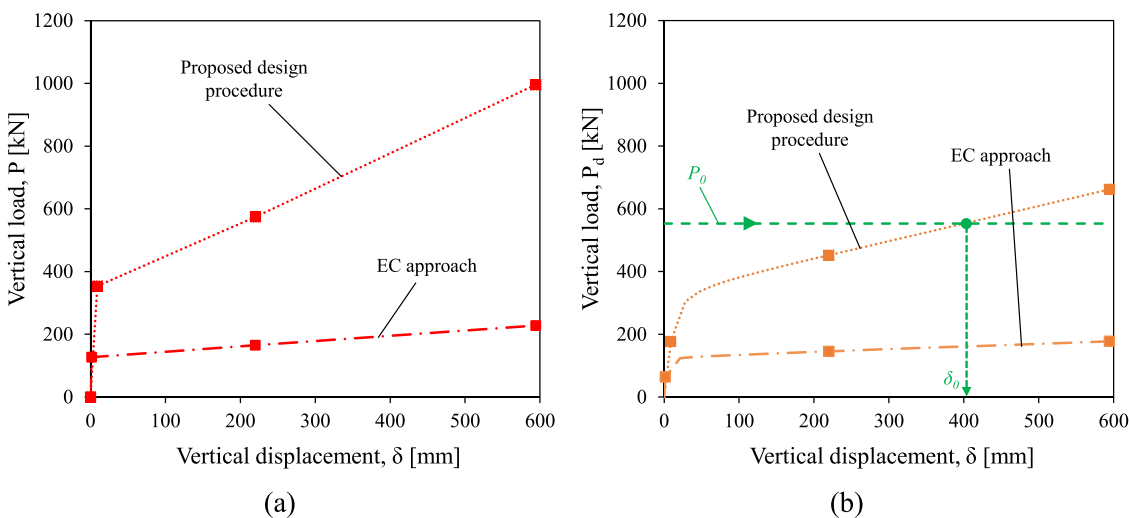


Fig. 10. Results from the comparisons between the proposed procedure and current Eurocodes design of tying reinforcement.

1. The Eurocodes does not provide the adequate intensity factor, i_f , (equal to 0.8 in *EC1* [5]), while for the proposed design procedure varies with the structural configuration, as discussed in [36,37], from 2.5 for beams to 3.125 for floor systems. Furthermore, the first

fundamental input parameter, the chord rotation capacity of the system – representative of the system’s ductility – must be also considered in the design of ties and lacks in the current Eurocodes.

2. The second fundamental input parameter, the dynamic amplification factor, is also not considered in Eurocodes. Indeed, the loss of load-bearing elements is a dynamic phenomenon and inertial effects must be adequately considered.

In the proposed procedure, both the chord rotation capacity and the dynamic amplification factor are adequately considered in the calculation and are adopted in the design of ties by using the Izzuddin & Sio proposal [36]. The example highlighted that: (i) the proposed procedure can design the adequate tying reinforcement, (ii) the current design provisions of Eurocodes [5,6] for tying reinforcement are not adequate, also according with previous studies [17,30,36,37,57–59].

4. Novel detailing for distributed ties in HC floors

A novel detailing for HC floor units is described for the distributed tying system with partially debonded strands and is proposed to optimize connections between the PC beams and the HC units. In particular,

the proposed detailing suggests placing distributed ties running along the longitudinal joints of HC units. Indeed, such option is considered more viable in construction practice compared with that with ties in voids, as already stated in the Section 2 of this work. The detailing is based on the observations of the example calculation previously reported, to meet practical construction issues and progressive collapse performance.

The section of the HC floor unit is reported in Fig. 11 where:

- Rebars are placed within the keyways of the HC slab with small diameter, usually 12 mm without robustness purposes, and are conservatively neglected in the calculation of the progressive collapse resistance.
- Strands are used for robustness scopes and are placed into longitudinal joints of the HC slab, along the whole span length.

Two options are shown, Option 1 (Fig. 11(a)) and 2 (Fig. 11(b)), both viable during manufacturing process. The observations are:

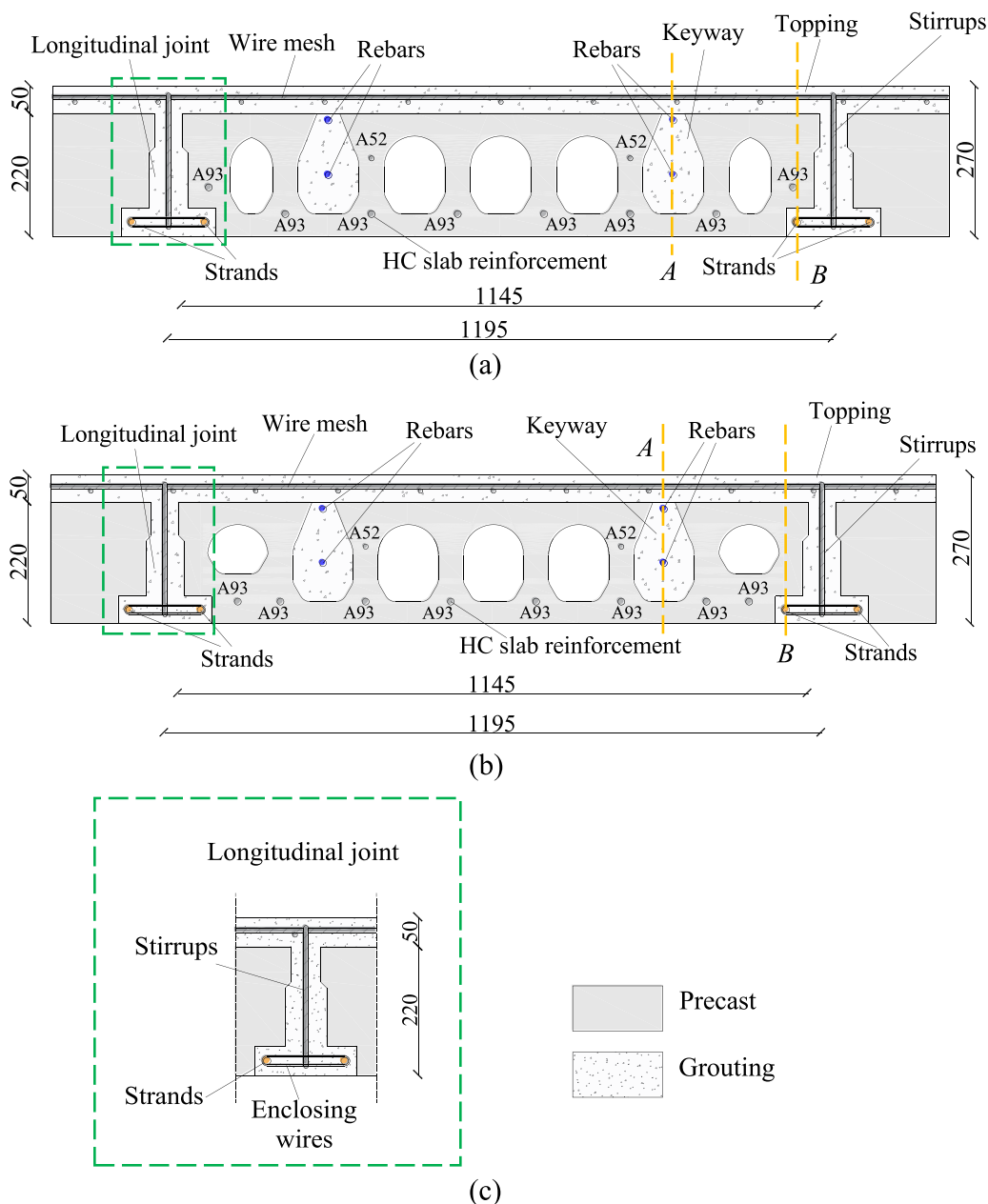


Fig. 11. Detailing of HC slab and joint: (a) Option 1, (b) Option 2, (c) detail of longitudinal joint. Dimensions in [mm].

- Openings at the base of the original *HC* section are provided to allow the passage of strands. The distributed floor ties composed of prestressed strands must be closed by small diameter wires to avoid the opening of joints at the large displacements.
- Stirrups should be placed into joints to connect the wire mesh placed in the concrete topping and the *HC* slab units.
- The strands placed into the longitudinal joints must be adequately placed approximately at the mid height of the opening to allow the correct concrete grouting. Generally, the indications provided by the Eurocode 2 [6] concerning the concrete cover should be followed, also regarding durability issues.
- The longitudinal joints (Fig. 11(c)) must be carefully designed and special attention should be paid to the stress concentration, expected to occur in correspondence of voids.

Fig. 12 shows the detailing for the two different options in correspondence of the Section A.

The following observations can be drawn:

- The rebars placed in the keyways must be well anchored to allow a sufficient integrity of the *HC* slab to the casted concrete. Both upper and lower rebars are placed to partially absorb the negative moment although *HC* slabs are usually designed as simply supported.
- In the case of an inverted *T*-shape beam, the placing of rebars is more complex compared to the usual *T*-shape section since a hole must be provided for the passage of ties.

Fig. 13 shows the detailing for the two different options in

correspondence of the Section B.

The following observations can be drawn:

- The strand is covered by a plastic tube in correspondence of the joint with the transversal *PC* beam. The plastic tube allows to overcome the issue of limited strand ductility. Indeed, such length is the debonded length L_{deb} used in this work to calculate the strand elongation in the analytical procedure. The remaining part of the strands outside the plastic tube are bonded.
- In the case of inverted *T*-beam cross section, a hole must be provided to allow the passage of the strand and the plastic tube across the joint.

5. Conclusions

In this work, a simple yet reliable robustness-oriented design procedure for tying reinforcement in precast concrete hollow-core floors is proposed. The work is based on the novel proposal by Izzuddin & Sio [36], where the chord rotation capacity and the dynamic amplification factor are estimated based on the recent analytical work by Ravasini [38]. The concept behind the proposed procedure is the optimisation of the amount tying reinforcement in *PC* buildings to meet construction practice and issues, with a sufficient margin of safety and accuracy, aimed to practicing engineers facing with the issue of mitigating progressive collapse phenomenon. An application example is provided to clarify the steps of the proposed procedure and a brief discussion on a novel detailing of ties in *HC* floor units is reported.

The following conclusions can be drawn:

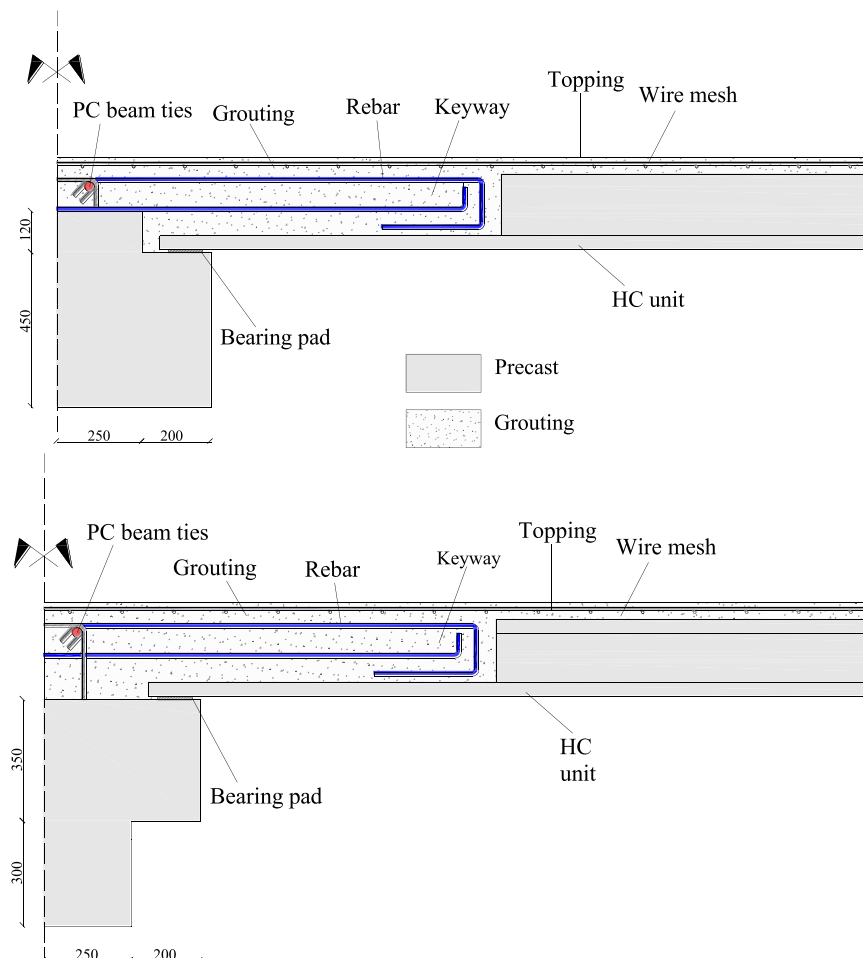


Fig. 12. Detailing of Section A. Dimensions in [mm].

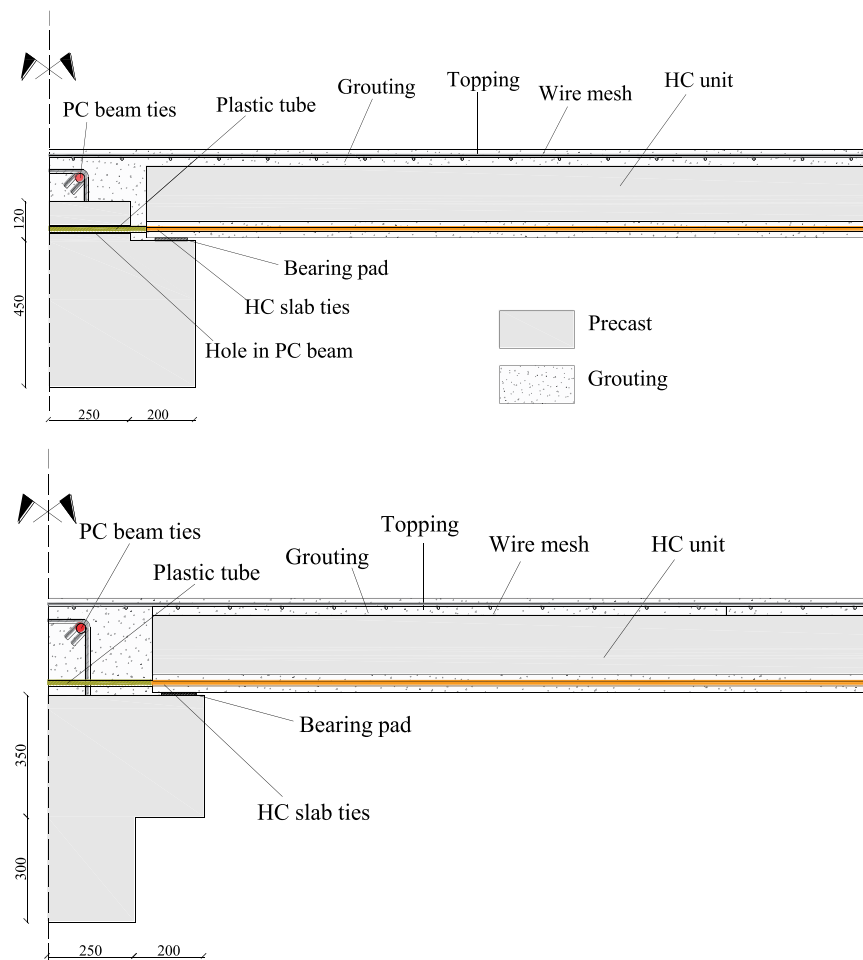


Fig. 13. Detailing of Section B: non-prestressed strand covered with plastic tube for debonding purposes for the two options. Dimensions in [mm].

- A novel proposal of using partially debonded strands is discussed and analytically investigated. To overcome the limited ductility of strands, an adequate debonding length, L_{deb} , above the support can be adopted. This choice is justified by the facts that strands provide high tensile resistance compared to rebars, by allowing lower reinforcement ratios and are easier to be arranged in HC floors. The ductility of the system can be governed by selecting the appropriate debonding length.
- The proposed procedure can be efficiently used to design tying reinforcement in precast concrete buildings, where the capacity of the system was demonstrated to be greater than the demand, with a rational optimisation of tying reinforcement placed in PC members. The importance of the system ductility - through the chord rotation capacity - and the dynamic amplification factor was highlighted. Indeed, lower system ductility and greater dynamic amplification factor lead to more punitive design, requiring higher amount of reinforcement.
- A step-by-step example is provided to clarify the design procedure, and finally the example demonstrated the inadequacy of the current design provisions of the Eurocodes, according also with other studies in the literature.
- The proposed detailing scheme presented in Section 4 could be experimentally tested and numerically investigated through detailed finite element analyses. It could be extended to other slab geometries for a wider application to structural robustness purposes. Also, the proposed detail is viable due to the possibility of control the manufacturing of the HC slabs during the extrusion process. In addition, based on construction practice, the filling of transversal

and longitudinal joints must be carried out and, therefore, it makes sense to provide the additional reinforcement within joints, with a reasonable increment of costs and workmanship. The cost and manufacturing aspects are interesting and are worth to be investigated in a dedicated work.

From the research point of view and future works, ad-hoc experimental campaigns are required to investigate the progressive collapse resistance at component and building levels with tying reinforcement, eventually coupled with detailed finite element simulations to further validate and refine the analytical calculations.

Declaration of Competing Interest

The authors declare that they have no known competing financial interests or personal relationships that could have appeared to influence the work reported in this paper.

Acknowledgements

Simone Ravasini would like to acknowledge Regione Emilia-Romagna, Italy, for sponsoring its doctoral programme at University of Parma, Italy, through the doctoral grant FSE 2018 Rif. PA D94J18000170007.

References

- [1] Adam JM, Parisi F, Sagaseta J, Lu X. Research and practice on progressive collapse and robustness of building structures in the 21st century. *Eng Struct* 2018;vol. 173: 122–49.
- [2] Russell JM, Sagaseta J, Cormie D, Jones AEK. Historical review of prescriptive design rules for robustness after the collapse of Ronan Point. *Structures* 2019;vol. 20(April):365–73.
- [3] Caredda G, Makoond N, Buitrago M, Sagaseta J, Chryssanthopoulos M, Adam JM. Learning from the progressive collapse of buildings. *Dev Built Environ* 2023;vol. 15 (July):100194.
- [4] DoD, Unified Facilities Criteria (UFC 4-023-03): Design of Buildings To Resist Progressive Collapse. Department of Defense, Washington DC, 2016.
- [5] CEN-EC1, “EN 1991-1-7: Eurocode 1 – actions on structures: general actions – accidental actions.” European Committee for Standardization, Brussels, 2006.
- [6] CEN-EC2, “EN 1992: Eurocode 2: Design of concrete structures - Part 1-1: General rules and rules for buildings.” European Committee for Standardization, Brussels, 2004.
- [7] fib Bulletin 63, “Design of precast concrete structures against accidental actions.” Lausanne, 2012.
- [8] Alshaiikh IMH, Abadel AA, Alrubaidi M. Precast RC structures’ progressive collapse resistance: current knowledge and future requirements. *Structures* 2022;vol. 37 (December 2021):338–52.
- [9] Kang SB, Tan KH. Robustness assessment of exterior precast concrete frames under column removal scenarios. *J Struct Eng* 2016;vol. 142(12).
- [10] Kang SB, Tan KH. Progressive collapse resistance of precast concrete frames with discontinuous reinforcement in the joint. *J Struct Eng* 2017;vol. 143(9):1–13.
- [11] Zhou Y, et al. Static load test on progressive collapse resistance of fully assembled precast concrete frame structure. *Eng Struct* 2019;vol. 200(September):109719.
- [12] Zhou Y, et al. Dynamic load test on progressive collapse resistance of fully assembled precast concrete frame structures. *Eng Struct* 2020;vol. 214(April): 110675.
- [13] Elsanadedy HM, Almusallam TH, Al-Salloum YA, Abbas H. Investigation of precast RC beam-column assemblies under column-loss scenario. *Constr Build Mater* 2017; vol. 142:552–71.
- [14] Kim SH, Do Kim H, Kang SM, Hwang HJ, Choi H. Effect of joint details on progressive collapse resistance of precast concrete structures. *J Build Eng* 2023;vol. 69(November 2022):106217.
- [15] Belleri A, Brunesi E, Nascimbene R, Pagani M, Riva P. Seismic performance of precast industrial facilities following major earthquakes in the Italian territory. *J Perform Constr Facil* 2015;vol. 29(5):04014135.
- [16] S. Ravasini and B. Belletti, “Construction method and numerical approach for the robustness of precast concrete buildings,” Published in fib Congress 2022, Oslo, 2022.
- [17] Scalvenzi M, Ravasini S, Brunesi E, Parisi F. Progressive collapse fragility of substandard and earthquake-resistant precast RC buildings. *Eng Struct* 2023;vol. 275:115242.
- [18] S. Ravasini, M. Scalvenzi, F. Parisi, B. Belletti, and A. Gasperi, “Role of structural details in progressive collapse of precast RC structures,” Proceedings of Italian Concrete Days 2020, 14–16 April, Naples, Italy, 2021, 2021.
- [19] Tohidi M, Baniotopoulos C. Effect of floor joint design on catenary actions of precast floor slab system. *Eng Struct* 2017;vol. 152:274–88.
- [20] Qian K, Li B. Investigation into resilience of precast concrete floors against progressive collapse. *Acids Struct J* 2019;vol. 116(2):171–82.
- [21] Qian K, Li B. Performance of precast concrete substructures with dry connections to resist progressive collapse. *J Perform Constr Facil* 2018;vol. 32(2):04018005.
- [22] PCA, “Design and construction of large-panel concrete structures - Suppl. Report A.” Portland Cement Association - Department of Housing and Urban Development, Washington DC, 1978.
- [23] Zhou Y, et al. Static load test on progressive collapse resistance of precast prestressed hollow core slabs. *J Struct Eng* 2023;vol. 149(2018):1–14.
- [24] Buitrago M, Nirvan M, Moragues JJ, Sagaseta J, Adam JM. Robustness of a full-scale precast building structure subjected to corner-column failure. *Structures* 2023;vol. 52(March):824–41.
- [25] Makoond N, Buitrago M, Adam JM. Tests on a full-scale precast building for robustness assessment. *Struct Congr 2023* 2023:1–11.
- [26] Zhou Y, et al. Reliability of fully assembled precast concrete frame structures against progressive collapse. *J Build Eng* 2022;vol. 51(February):104362.
- [27] Lin K, Chen Z, Li Y, Lu X. Uncertainty analysis on progressive collapse of RC frame structures under dynamic column removal scenarios. *J Build Eng* 2022;vol. 46 (December 2021):103811.
- [28] Tohidi M, Janby A. Finite-element modeling of progressive failure for floor-to-floor assembly in the precast cross-wall structures. *J Struct Eng* 2020;vol. 146(6): 04020087.
- [29] S.M. Miratashiyazdi, “Robustness of Steel Framed Buildings With Pre-Cast Concrete Floor Slabs,” PhD Thesis - University of Manchester, 2014.
- [30] Ravasini S, Belletti B, Brunesi E, Nascimbene R, Parisi F. Nonlinear dynamic response of a precast concrete building to sudden column removal. *Appl Sci* 2021; vol. 11(2):1–22.
- [31] Alanani M, Ehab M, Salem H. Progressive collapse assessment of precast prestressed reinforced concrete beams using applied element method. *Case Stud Constr Mater* 2020;vol. 13:e00457.
- [32] Mucedero G, Brunesi E, Parisi F. Progressive collapse resistance of framed buildings with partially encased composite beams. *J Build Eng* 2021;vol. 38(January): 102228.
- [33] Makoond N, Buitrago M, Adam JM. Computational study on the progressive collapse of precast reinforced concrete structures. *Curr Perspect N Dir Mech, Model Des Struct Syst* 2022:187–8.
- [34] Tohidi M, Yang J, Baniotopoulos C. Numerical evaluations of codified design methods for progressive collapse resistance of precast concrete cross wall structures. *Eng Struct* 2014;vol. 76:177–86.
- [35] Tohidi M, Janby A. Finite-element modeling of progressive failure for floor-to-floor assembly in the precast cross-wall structures. *J Struct Eng* 2020;vol. 146(6): 04020087.
- [36] Izzuddin BA, Sio J. Rational horizontal tying force method for practical robustness design of building structures. *Eng Struct* 2022;vol. 252(February):113676.
- [37] Ravasini S, Sio J, Franceschini L, Izzuddin BA, Belletti B. Validation of simplified tying force method for robustness assessment of RC framed structures. *Eng Struct* 2021;vol. 249(October):113291.
- [38] Ravasini S. An analytical framework for the evaluation of the progressive collapse resistance of precast concrete hollow-core floors. *J Build Eng* 2023;vol. 80 (November):108061.
- [39] Azim I, Yang J, Bhatta S, Wang F, Feng Liu Q. Factors influencing the progressive collapse resistance of RC frame structures. *J Build Eng* 2020;vol. 27(April 2019): 100986.
- [40] Guaygua B, Sánchez-Garrido AJ, Yepes V. A systematic review of seismic-resistant precast concrete buildings. *Structures* 2023;vol. 58(September).
- [41] Li S, Wang H, Liu H, Shan S, Zhai C. Experimental study on progressive collapse of self-centering precast concrete frame with infill walls. *Eng Struct* 2023;vol. 294 (April):116746.
- [42] Yang XJ, Lin F, Gu XL. Experimental study on a novel method to improve progressive collapse resistance of RC frames using locally debonded rebars. *J Build Eng* 2021;vol. 41(October 2020):102428. <https://doi.org/10.1016/j.jobe.2021.102428>.
- [43] M. Tohidi, “Effect of floor-to-floor joint design on the robustness of precast concrete cross wall buildings.” PhD Thesis, University of Birmingham, 2015.
- [44] Sarkis AI, Sullivan TJ, Brunesi E, Nascimbene R. Investigating the effect of bending on the seismic performance of hollow-core flooring. *Int J Concr Struct Mater* 2023; vol. 17(1):1–12.
- [45] Fédération Internationale du Béton (fib), fib Model Code for Concrete Structures 2010. Lausanne, Switzerland, 2013.
- [46] Yu J, Tan KH. Structural behavior of RC beam-column subassemblages under a middle column removal scenario. *J Struct Eng* 2013;vol. 139(2):233–50.
- [47] Rankin GIB, Long AE. Arching action strength enhancement in laterally-restrained slab strips. *Proc Inst Civ Eng: Struct Build* 1997;vol. 122(4):461–7.
- [48] El Debs MK, Miotto AM, El Debs ALHC. Analysis of a semi-rigid connection for precast concrete. *Proc Inst Civ Eng: Struct Build* 2010;vol. 163(1):41–51.
- [49] Elliott KS, Davies G, Ferreira M, Gorgun H, Mahdi AA. Can precast concrete structures be designed as semi-rigid frames? Part 1 - the experimental evidence. *Struct Eng* 2003;vol. 81(16):14–27.
- [50] Elliott KS, Davies G, Ferreira M, Gorgun H, Mahdi AA. Can precast concrete structures be designed as semi-rigid frames? Part 2 - analytical equations & column effective length factors. *Struct Eng* 2003;vol. 81(16):28–37.
- [51] fib Bulletin 43, “Structural connections for precast concrete buildings.” Lausanne, 2008.
- [52] Feng DC, Xu J. An efficient fiber beam-column element considering flexure-shear interaction and anchorage bond-slip effect for cyclic analysis of RC structures. *Bull Earthq Eng* 2018;vol. 16(11):5425–52.
- [53] Izzuddin BA, Vlassis AG, Elghazouli AY, Nethercot DA. Progressive collapse of multi-storey buildings due to sudden column loss - part I: simplified assessment framework. *Eng Struct* 2008;vol. 30(5):1308–18.
- [54] Vlassis AG, Izzuddin BA, Elghazouli AY, Nethercot DA. Progressive collapse of multi-storey buildings due to sudden column loss-part II: application. *Eng Struct* 2008;vol. 30(5):1424–38.
- [55] Izzuddin BA, Nethercot DA. Design-oriented approaches for progressive collapse assessment: load-factor vs ductility-centred methods. *Proc 2009 Struct Congr - Don't Mess Struct Eng* 2009:1791–800.
- [56] CEN-ECO, “EN 1990 Eurocode 0: Basis of structural design.” European Committee for Standardization, Brussels, 2002.
- [57] Li Y, Lu X, Guan H, Ye L. An improved tie force method for progressive collapse resistance design of reinforced concrete frame structures. *Eng Struct* 2011;vol. 33 (10):2931–42.
- [58] Qian K, Li B. Research advances in design of structures to resist progressive collapse. *J Perform Constr Facil* 2015;vol. 29(5):1–11.
- [59] Belletti B, Franceschini L, Ravasini S. Tie force method for reinforced concrete structures. *Proc Int Fib Symp Concept Des Struct* 2019:57–64.